Journal of Computational Physics 229 (2010) 7042–7057

Contents lists available at ScienceDirect

Journal of Computational Physics

journal homepage: www.elsevier.com/locate/jcp

Explicit and implicit finite difference schemes for fractional Cattaneo equation

H.R. Ghazizadeh [a], M. Maerefat [a,*], A. Azimi [b]

[a] Dept. Mech. Eng., Tarbiat Modares University, P.O. Box 14115-143, Tehran, Iran
[b] Dept. Mech. Eng., Shahid Chamran University of Ahvaz, Ahvaz, Iran

ARTICLE INFO

Article history:
Received 28 February 2010
Received in revised form 25 May 2010
Accepted 25 May 2010
Available online 31 May 2010

Keywords:
Fractional Cattaneo equation
Finite difference schemes
Stability
Convergence rate

ABSTRACT

In this paper, the numerical solution of fractional (non-integer)-order Cattaneo equation for describing anomalous diffusion has been investigated. Two finite difference schemes namely an explicit predictor–corrector and totally implicit schemes have been developed. In developing each scheme, a separate formulation approach for the governing equations has been considered. The explicit predictor–corrector scheme is the fractional generalization of well-known MacCormack scheme and has been called Generalized MacCormack scheme. This scheme solves two coupled low-order equations and simultaneously computes the flux term with the main variable. Fully implicit scheme however solves a single high-order undecomposed equation. For Generalized MacCormack scheme, stability analysis has been studied through Fourier method. Through a numerical test, the experimental order of convergency of both schemes has been found. Then, the domain of applicability and some numerical properties of each scheme have been discussed.

© 2010 Elsevier Inc. All rights reserved.

1. Introduction

In recent years, the validity of using standard diffusive constitutive models such as Fourier or Fick's law has been questioned extensively. The main reason returns to the underlying physical deficiency of these models which consider infinite speed for propagation of a diffusive quantity such as temperature or mass in the medium. In order to consider the finite velocity of propagation, several new constitutive models have been introduced. Among them, Cattaneo model has been used very extensively in modelling both heat and mass transfer [1–4]. However, it has been experimentally observed in many natural systems that diffusive processes behave anomalously [5]; i.e. mean-square-displacement (MSD) in these complex systems does not follow standard linear behaviour and takes the form MSD = Kt^{α}, where α is the anomalous diffusion exponent. This anomalous behaviour has been recently described through the fractional generalization of classical Cattaneo model as a phenomenological constitutive equation in the following 1-D form [5]:

$$f(x,t)+\tau^{\alpha}\frac{\partial^{\alpha}f(x,t)}{\partial t^{\alpha}}=-D\frac{\partial u(x,t)}{\partial x},\quad 0<\alpha\leqslant 1, \tag{1}$$

where τ is the relaxation time, D is the diffusion constant, f is the flux, u is the diffusing quantity and $\partial^{\alpha}/\partial t^{\alpha}$ is the fractional (non-integer) time derivative based on Riemann–Liouville definition. For $\alpha = 1$, Eq. (1) reduces to standard Cattaneo model and for the limiting case of $\alpha \to 0$ (or $\tau = 0$), classical diffusive models of Fourier or Fick law are recovered. Combining Eq. (1) with continuity equation:

* Corresponding author. Tel.: +98 21 82883360; fax: +98 21 82883381.
E-mail address: Maerefat@modares.ac.ir (M. Maerefat).

0021-9991/$ - see front matter © 2010 Elsevier Inc. All rights reserved.
doi:10.1016/j.jcp.2010.05.039

$$\frac{\partial u(x,t)}{\partial t} = -\frac{\partial f(x,t)}{\partial x}, \tag{2}$$

results in the generalized Cattaneo equation:

$$\frac{\partial u(x,t)}{\partial t} + \tau^{\alpha}\frac{\partial^{1+\alpha} u(x,t)}{\partial t^{1+\alpha}} = D\frac{\partial^2 u(x,t)}{\partial x^2}. \tag{3}$$

Recently, Eq. (1) has been used as a constitutive equation for deriving a pseudo-heterogeneous model for describing the reaction–diffusion problem in a disordered porous medium by using the method of volume averaging [6]. Using fractional calculus in different fields of science and engineering specially those related to diffusion in porous medium is growing very rapidly [7–9]. One of the main reasons is its great ability in describing the memory and hereditary properties of the system. Consequently, developing new and efficient numerical schemes for solving Fractional Partial Differential Equations (FPDEs) has been the target of recent investigations in numerical analysis. One possible classification of FPDEs is space and time-fractional diffusion models. Since Eq. (3) falls in time-fractional diffusion equations (TFDEs), we focus on recent investigations concerning numerical approximation of time FPDEs. Langlands and Henry [10] investigated TFDEs using an implicit and unconditionally stable numerical scheme based on L1 scheme introduced in [11]. Yuste and Acedo [12] employed Grünwald–Letnikov definition of fractional derivative and developed an explicit scheme and found the stability condition through Von Neumann stability criterion. Yuste [13] extended their previous work and developed a so called weighted average difference scheme which in contrast to their previous work [12] which was conditionally stable, may become unconditionally stable by choosing a proper weighting parameter. By using spectral method, Lin and Xu [14] first discretized the time-fractional derivative based on the Caputo definition and then developed an implicit and unconditionally stable scheme for solving TFDEs. Time fractional Fokker–Plank equation has been solved numerically in [15] by using a predictor–corrector approach. The author actually increased the accuracy and reduced the cost of previously introduced predictor–corrector schemes [16,17] by changing the numerical approximation in predictor formula. In [18], based on the Grünwald–Letnikov definition, a fully implicit scheme has been developed. Then, by using Fourier stability analysis, it has been shown that the implicit scheme is unconditionally stable. Scherer et al. [19] employed Grünwald–Letnikov scheme for numerically solving the fractional heat equation used for modelling heat transfer in a specific porous medium. They developed a general formulation consisting of explicit, implicit and fully implicit schemes and studied the stability and accuracy of the proposed methods. In [20], a new discretization based on numerically approximating the Caputo definition has been proposed for $0 < \alpha < 1$. Again, by using Grünwald–Letnikov definition for approximating time fractional derivative, Cui [21] successfully increased the spatial accuracy by using a compact finite difference.

In the present paper, by using the concept of single-phase lag equation [22] and the recently introduced fractional Taylor series expansion formula [23], we first derive the generalized Cattaneo model based on Caputo time fractional definition which enables us to use traditional initial conditions. Then, we investigate the numerical solution of the generalized Cattaneo equation by developing two explicit and implicit schemes. The explicit predictor–corrector scheme is the fractional generalization of the well-known MacCormack scheme for solving hyperbolic equations and is called Generalized MacCormack (GMcC) scheme. In developing these two schemes, we have used two different approaches. GMcC scheme has been developed for solving two coupled lower-order equations; however for fully implicit (FI) scheme, single higher-order equation is solved. Former approach has been called lower-order approach (LOA) while the latter is called higher-order approach (HOA). As we will see, this simple idea of LOA offers us great gains and opens new directions for using higher-order explicit schemes for solving anomalous diffusion equations. Finally, the range of applicability and also some numerical properties of both schemes such as stability and experimental order of convergency are studied through numerical tests.

2. Caputo-based generalized Cattaneo equation

Several definitions of a fractional derivative have been proposed, for example the definitions of Riemann–Liouville, Grünwald–Letnikov and Caputo [7]. From the historical point of view, Riemann–Liouville definition seems to be the most important definition among the others, because many of the later achievements of fractional calculus have come from this definition. Caputo definition enables us to use initial/boundary conditions of practical type in the formulation. In the present study initial conditions of practical type are of interest since fractional derivative has been applied in time domain. Also it has the advantage of employing the classical Laplace transform for fractional derivatives which is very useful in deriving the analytic solution. In other words, Riemann–Liouville definition is more preferred in pure mathematics, but not in applied and engineering problems which involve standard definitions for initial/boundary conditions. For this reason, Caputo definition is preferred in modeling practical problems. On the other hand, Grünwald–Letnikov definition serves as an efficient definition for numerical approximation of a fractional derivative based on Riemann–Liouville definition, since these two definitions are equivalent for a wide class of functions. These three definitions are defined as [7]:

$$\text{Riemann—Liouville}: {}_0D^{\alpha}_{R-L} f(t) \equiv \frac{d^{\alpha} f}{dt^{\alpha}} \equiv \frac{1}{\Gamma(m-\alpha)}\frac{\partial^m}{\partial t^m}\int_0^t \frac{f(\tau)}{(t-\tau)^{\alpha+1-m}}\,d\tau, \quad m-1 \leqslant \alpha < m, \quad m \in N, \tag{4}$$

$$\text{Grunwald–Letnikov}: D^{\alpha}f(t) \equiv \frac{d^{\alpha}f}{dt^{\alpha}} \equiv \frac{1}{\Delta t^{\alpha}} \sum_{k=0}^{[t/\Delta t]} \omega_k^{\alpha} f(t-k\Delta t), \quad \text{where} \quad \omega_k^{\alpha} = (-1)^k \binom{\alpha}{k} \tag{5}$$

$$\text{Caputo}: D_*^{\alpha}f(t) \equiv \frac{d^{\alpha}f}{dt^{\alpha}} \equiv \frac{1}{\Gamma(m-\alpha)} \int_0^t \frac{f^{(m)}(\tau)}{(t-\tau)^{\alpha+1-m}} d\tau, \quad m-1 < \alpha < m, \quad m \in N, \tag{6}$$

The difference between Caputo and Riemann–Liouville definition is

$$D_*^{\alpha}f(t) - D_{R-L}^{\alpha}f(t) = -\sum_{k=0}^{m-1} \frac{t^{k-\alpha}}{\Gamma(k+1-\alpha)} f^{(k)}(0), \quad m-1 < \alpha \leqslant m. \tag{7}$$

We aim to derive generalized Cattaneo Eq. (1) based on Caputo definition. To do this, we get help from the well-established concept of phase (time)-lagging in the field of heat transfer. As it is mentioned in [22] and the references cited therein, classical Cattaneo constitutive model ($\alpha = 1$ in Eq. (1)) can be derived directly through Taylor series expansion of the single-phase-lag delayed constitutive relation $f(x,t+\tau) = -D\partial u/\partial x$ up to first order. In the same way, in order to arrive at *fractional* Cattaneo model (1), instead of expanding single-phase-lag delayed equation $f(x,t+\tau) = -D\partial u/\partial x$ by classical Taylor formula, we expand it up to first order through the recently introduced *fractional* Taylor formula [23] in the following form:

$$f(x,t+\tau) \simeq f(x,t) + \frac{\tau^{\alpha}}{\Gamma(1+\alpha)} \frac{\partial^{\alpha} f(x,t)}{\partial t^{\alpha}} = -D\frac{\partial u(x,t)}{\partial x}, \quad 0 < \alpha \leqslant 1. \tag{8}$$

Without losing the generality we can merge $\Gamma(1+\alpha)$ in τ^{α} which results in:

$$f(x,t) + \tau^{\alpha} \frac{\partial^{\alpha} f(x,t)}{\partial t^{\alpha}} = -D\frac{\partial u(x,t)}{\partial x}, \quad 0 < \alpha \leqslant 1. \tag{9}$$

Therefore, from Eq. (9) it is clear that Eq. (1) is rederived but this time the time-fractional operator in Eq. (9) is based on Caputo definition because, the fractional Taylor series which is applied for the derivation of Eq. (9) is valid only with Caputo definition [23].

Then, by combining Eq. (9) with Eq. (2) we arrive at generalized Cattaneo equation based on Caputo definition:

$$\frac{\partial u(x,t)}{\partial t} + \tau^{\alpha} \frac{\partial^{1+\alpha} u(x,t)}{\partial t^{1+\alpha}} = D\frac{\partial^2 u(x,t)}{\partial x^2}. \tag{10}$$

Therefore, the generalized Cattaneo model in the sense of Riemann–Liouville definition is now transformed to generalized Cattaneo model in the sense of Caputo definition through applying the fractional Taylor series formula on the single-phase-lag constitutive equation $f(x,t+\tau) = -D\partial u/\partial x$.

In summary, the governing equations of this paper are Eqs. 2, 9, 10. For the GMcC scheme, two coupled equations of (2) and (9) are solved simultaneously while for FI scheme, a single Eq. (10) is solved. Also, all the time-fractional operators in these three equations are now defined based on Caputo derivative.

3. Generalized MacCormack scheme

As mentioned in the introduction, the formulation of GMcC scheme, in contrast to the FI scheme, is based on the idea of LOA, i.e. solving a set of coupled time-fractional equations. So, for introducing GMcC scheme, we first formulate it for the case of a scalar (single) time-fractional equation. This single time-fractional equation serves as a *model* equation for LOA formulation of generalized Cattaneo equation. Then the stability of the derived scheme is analyzed using the Von Neumann stability criterion. Then, the results of the discussion made for a single time-fractional equation are extended for the case of systems of time-fractional equations. The extension is made rather easily and allows us not be involved in the complexities of applying GMcC scheme directly for systems of equations. This approach is very common in developing numerical schemes and studying their numerical properties for the well-known system of hyperbolic equations such as Euler, shallow water and thermal wave equations.

And finally, the formulation of GMcC scheme for the generalized Cattaneo equation is presented in the next section as a special case of systems of time-fractional equations.

3.1. Generalized MacCormack scheme for a scalar time fractional conservation equation

Consider the following scalar time-fractional equation:

$$\frac{\partial^{\alpha} u}{\partial t^{\alpha}} + \frac{\partial f(u)}{\partial x} = 0.0, \tag{11}$$

where u and f are called scalar conserved quantity and scalar flux function, respectively. Eq. (11) can be called scalar time-fractional conservation equation and for the special case of $\alpha = 1$, it reduces to classical scalar conservation equation. Eq. (11) serves as the model equation for systems of time-fractional conservation equations.

First, for some positive integers N and M let:

$$t_n = n\Delta t \quad n = 0, 1, \ldots, N,$$

and

$$x_i = j\Delta x, \quad j = 0, 1, \ldots, M,$$

where the grid sizes in time and space are defined respectively by $\Delta t = T/N$ and $\Delta x = L/M$.

As mentioned before, Grünwald–Letnikov definition serves as the numerical approximation of Riemann–Liouville definition. However, the time-fractional operator in Eq. (11) is based on Caputo definition. In order to employ Grünwald–Letnikov definition for discretization of time-fractional operator in Eq. (11), we see from Eq. (7) that for $0 < \alpha \leqslant 1$, the difference between Caputo and Riemann–Liouville definitions contains only one term and depends only on the initial condition $f(t{=}0)$. Therefore, if $u(x, t = 0)$ in Eq. (11) is small, we can employ Grünwald–Letnikov definition for numerical approximation of time-fractional operator in Eq. (11). The most favorable case happens under the homogeneous initial conditions when all the three definitions become equivalent. Therefore, for developing the generalized MacCormack scheme, without losing the generality, we assume that all initial conditions of the problem are zero.

According to the definition of Grünwald–Letnikov scheme for time fractional derivatives Eq. (5) and knowing that $\omega_0^\alpha = 1.0$, the *generalized* MacCormack scheme for Eq. (11) is formulated as

Predictor:

$$\bar{u}_j^{n+1} = -\sum_{k=1}^{n+1} \omega_k^\alpha u_j^{n+1-k} - \frac{\Delta t^\alpha}{\Delta x}\left(f_{j+1}^n - f_j^n\right), \tag{12}$$

and

Corrector:

$$u_j^{n+1} = \frac{1}{2}\left[-\sum_{k=1}^{n+1} \omega_k^\alpha u_j^{n+1-k} - \frac{\Delta t^\alpha}{\Delta x}\left(\bar{f}_j^{n+1} - \bar{f}_{j-1}^{n+1}\right) + \bar{u}_j^{n+1}\right], \tag{13}$$

where the variables with over bar are predicted values calculated from Eq. (12). As can be seen from Eq. (12), space derivative is discretized forward while in the corrector formula (13) it is discretized backward. In using the classical MacCormack scheme for hyperbolic equations ($\alpha = 1$ in Eq. (11)), according to the direction of the wave propagation, the order of discretizing can be reversed, but in the present study the mentioned order has lead to better results. By setting $\alpha = 1.0$ in Eqs. (12) and (13), classical MacCormack scheme for hyperbolic equations is obtained. We have sought the rate of convergency of the generalized MacCormack scheme through numerical tests and found that GMcC scheme has second-order spatial rate of convergency and $(1 + \alpha)$ as the temporal rate of convergency. The detailed results are presented in Section 5.

3.1.1. Stability analysis

In this section, by using Von Neumann stability criterion for fractional partial differential equations [18], we analyze the stability of GMcC scheme. In order to analyze the stability of MacCormack scheme (12) and (13) for scalar time-fractional conservation Eq. (11), we should find a choice for the flux function $f(u)$. To do this, one simple possible choice is $f(u) = cu$ where $c = const$ which leads to linear time-fractional equation. This choice, as will be shown later, will enable us to easily extend the results of the stability analysis for a *scalar* time-fractional conservation equation to *system* of time-fractional conservation equations. This is a very established approach in studying hyperbolic equations which has been employed in the present study as an idea to be used for time-fractional conservation equations.

First, by setting $f(u) = cu$ and through inserting the predicted values from Eq. (12) into Eq. (13) and after some mathematical manipulation, we arrive at the following equation:

$$u_j^{n+1} = -\sum_{k=1}^{n+1} \omega_k^\alpha u_j^{n+1-k} - \frac{1}{2}\frac{c\Delta t^\alpha}{\Delta x}\left[-\sum_{k=1}^{n+1} \omega_k^\alpha u_j^{n+1-k} + \sum_{k=1}^{n+1} \omega_k^\alpha u_{j-1}^{n+1-k} + u_{j+1}^n - u_j^n\right] + \frac{1}{2}\frac{c^2\Delta t^{2\alpha}}{\Delta x^2}\left[u_{j+1}^n - 2u_j^n + u_{j-1}^n\right]. \tag{14}$$

Letting:

$$\varepsilon_j^n = u_j^n - U_j^n,$$

where U_j^n is the approximate solution of Eq. (14), the corresponding roundoff error equation is obtained:

$$\varepsilon_j^{n+1} = -\sum_{k=1}^{n+1} \omega_k^\alpha \varepsilon_j^{n+1-k} - \frac{1}{2}\frac{c\Delta t^\alpha}{\Delta x}\left[-\sum_{k=1}^{n+1} \omega_k^\alpha \varepsilon_j^{n+1-k} + \sum_{k=1}^{n+1} \omega_k^\alpha \varepsilon_{j-1}^{n+1-k} + \varepsilon_{j+1}^n - \varepsilon_j^n\right] + \frac{1}{2}\frac{c^2\Delta t^{2\alpha}}{\Delta x^2}\left[\varepsilon_{j+1}^n - 2\varepsilon_j^n + \varepsilon_{j-1}^n\right]. \tag{15}$$

For analyzing the stability of the algorithm, we can assume that the solution of Eq. (15) can be written in the form of $\varepsilon_j^n = C_n e^{i\phi j\Delta x}$ where the C_n are the Fourier series coefficients of ε_j^n and $i = \sqrt{-1}$. The linear stability condition is satisfied as long as G does not grow as time goes to infinity, i.e. $G = |C_n/C_0| \leqslant 1$ for all n.

Inserting $\varepsilon_j^n = C_n e^{i\phi j\Delta x}$ in Eq. (15) and setting $v_\alpha = c\Delta t^\alpha/\Delta x$ and after some mathematical manipulation, we have:

$$C_{n+1} = C_n\left[-\omega_1^\alpha - \frac{1}{2}v_\alpha\left(\omega_1^\alpha(-1+\cos(\phi\Delta x) - i\sin(\phi\Delta x)) + \cos(\phi\Delta x) + i\sin(\phi\Delta x) - 1\right)\right] + \left[-\sum_{k=2}^{n+1}\omega_k^\alpha C_{n+1-k} - \frac{1}{2}v_\alpha\left(-\sum_{k=2}^{n+1}\omega_k^\alpha C_{n+1-k} + \sum_{k=2}^{n+1}\omega_k^\alpha C_{n+1-k}(\cos(\phi\Delta x) - i\sin(\phi\Delta x))\right)\right] + C_n v_\alpha^2(\cos(\phi\Delta x) - 1). \tag{16}$$

Theorem 1. *The generalized MacCormack scheme (12) and (13) is stable if* $v_\alpha \leqslant 1$.

Proof. In order to prove Theorem 1, we use mathematical induction as follows. For $n = 0$, the last bracket in Eq. (16) vanishes and by considering $\omega_1^\alpha = -\alpha$, after some trigonometric simplifications we obtain:

$$\left|\frac{C_1}{C_0}\right| = \left|\left(\alpha - v_\alpha\sin^2(\beta/2)(\alpha - 1 + 2v_\alpha)\right) - i\frac{v_\alpha\sin(\beta)}{2}(\alpha+1)\right|, \tag{17}$$

where $\beta = \phi\Delta x$.

By plotting the amplification factor $|C_l/C_0| \leqslant 1$ with respect to v_α, we will find that $G_0 \leqslant 1$ holds as long as $v_\alpha \leqslant 1$. Fig. 1 shows the validity of this statement for some values of α. It is obvious from Fig. 1 that for different values of α, the magnitude of the amplification factor remains less than or equal 1 only for $v_\alpha \leqslant 1$. As v_α becomes greater than 1, i.e. $v_\alpha = 1.1$ in Fig. 1, the magnitude of the amplification factor extends that of *unit* circle which is the stability margin. In other words, it violates the stability criterion $G_0 \leqslant 1$ for the values of v_α greater than 1.

Being valid for the case of $n = 0$ under the condition of $v_\alpha \leqslant 1$, we assume that $|C_l/C_0| \leqslant 1$ is valid for $l = 1,\ldots,n$ under the same condition i.e. $v_\alpha \leqslant 1$. Returning back to Eq. (16), we rewrite it in the following form:

$$\begin{aligned} &C_{n+1} = d_1 C_n - d_2\sum_{k=2}^{n+1}\omega_k^\alpha C_{n+1-k}, \quad |C_l| \leqslant |C_0|(l = 1,\ldots,n)\\ &d_1 = -\omega_1^\alpha - \frac{1}{2}v_\alpha\left(\omega_1^\alpha(-1+\cos(\beta) - i\sin(\beta)) + \cos(\beta) + i\sin(\beta) - 1\right) + v_\alpha^2(\cos(\beta) - 1),\\ &d_2 = 1 + \frac{1}{2}v_\alpha(-1+\cos(\beta) - i\sin(\beta)). \end{aligned} \tag{18}$$

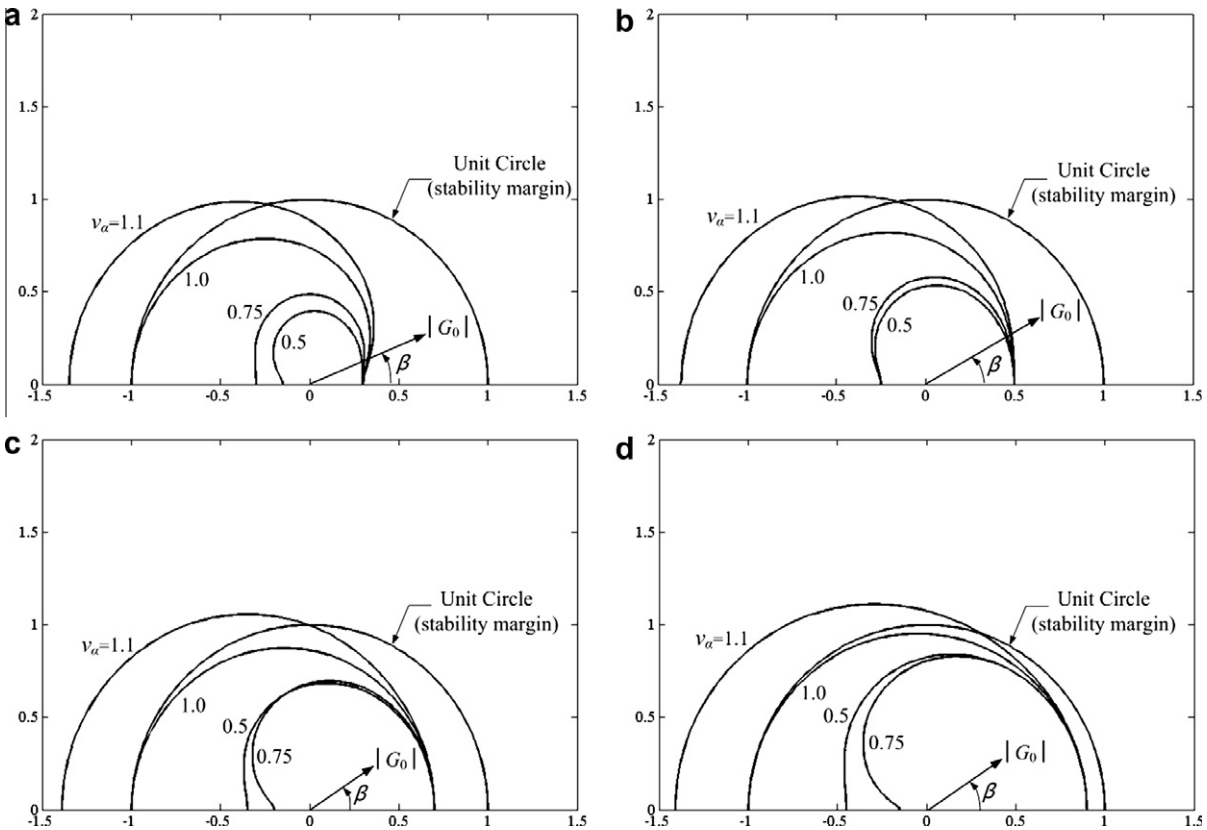

Fig. 1. Polar plot of G_0 modulus: (a) $\alpha = 0.3$, (b) $\alpha = 0.5$, (c) $\alpha = 0.7$, and (d) $\alpha = 0.9$.

Now, by using the properties of the coefficients described in Lemma 1 of Ref. [18], we have:

$$C_{n+1} \leqslant d_1 C_n - d_2 \sum_{k=2}^{n+1} \omega_k^{\alpha} C_{n+1-k},$$

$$C_{n+1} \leqslant \left[d_1 - d_2 \sum_{k=2}^{n+1} \omega_k^{\alpha}\right] C_0 = \left[d_1 - d_2\left(\sum_{k=2}^{n+1} \omega_k^{\alpha} - \omega_1^{\alpha}\right)\right] C_0 = \left[d_1 - d_2\left(\sum_{k=2}^{n+1} \omega_k^{\alpha} + \alpha\right)\right] C_0 \leqslant \left[d_1 + d_2\left(-\sum_{k=2}^{n+1} \omega_k^{\alpha} - \alpha\right)\right] C_0,$$

$$\left|\frac{C_{n+1}}{C_0}\right| \leqslant |d_1 + d_2(1-\alpha)|, \tag{19}$$

If we replace the relations for d_1 and d_2 from Eq. (18) in the last inequality of Eq. (19) we obtain:

$$G = \left|\frac{C_{n+1}}{C_0}\right| \leqslant \left|-v_\alpha i \sin(\beta) + 1 + v_\alpha^2(\cos(\beta) - 1) + \frac{1}{2} v_\alpha \cos(\beta)\right|. \tag{20}$$

Therefore in order to complete the mathematical induction, we should show that the inequality of Eq. (20) is valid under the condition of $v_\alpha \leqslant 1$ like for the case of $n = 0$. Since, amplification factor $G = |C_{n+1}/C_0|$ in Eq. (20) depends only on v_α and β, and does not depend on α explicitly, therefore the polar plots of amplification factor with respect to v_α is the same for all α. For this reason, only the plot of amplification factor G for a typical value of α i.e. 0.8 is given which is the same for other values of α. From Fig. 2 we find that $G = |C_{n+1}/C_0| \leqslant 1$ holds only under the condition of $v_\alpha \leqslant 1$ i.e. the same condition of the case $n = 0$. In other words, the magnitude of the amplification factor for $v_\alpha = 1$ coincides with the unit circle and for $v_\alpha < 1$ remains inside the unit circle which is the stability margin. Thus, mathematical induction is complete and Theorem 1 is proved. □

3.2. Generalized MacCormack scheme for systems of time fractional conservation equations

In the previous section, we formulated the GMcC scheme for a scalar time-fractional conservation equation and investigated its stability through Von Neumann stability criterion. In this section, we extend the discussions of the previous section for systems of time-fractional conservation equations. Consider the following systems of time-fractional conservation equations:

$$\frac{\partial^{\boldsymbol{\alpha}} \boldsymbol{E}}{\partial t^{\boldsymbol{\alpha}}} + \frac{\partial \boldsymbol{F}}{\partial x} = \boldsymbol{0}, \tag{21}$$

where vectors $\boldsymbol{E} = \begin{bmatrix} E_1 \\ \vdots \\ E_m \end{bmatrix}$, $\boldsymbol{F} = \boldsymbol{F}(\boldsymbol{E}) = \begin{bmatrix} F_1 \\ \vdots \\ F_m \end{bmatrix}$ and $\boldsymbol{\alpha} = \begin{bmatrix} \alpha_1 \\ \vdots \\ \alpha_m \end{bmatrix}$ are the vector of conserved variable, flux and order of differentiation, respectively. m is the number of coupled time-fractional equations. We find that the difference between systems of time-fractional Eq. (21) with scalar time-fractional conservation Eq. (11) is that the *scalar* quantities for conserved variable u and flux f in (11) is now replaced by *vector* of conserved variables and flux functions.

Now, we formulate GMcC scheme for system of Eq. (21) in the following form:

Predictor:

$$\widetilde{\boldsymbol{E}}_j^{n+1} = -\sum_{k=1}^{n+1} \omega_k^{\boldsymbol{\alpha}} \boldsymbol{E}_j^{n+1-k} - \frac{\Delta t^{\boldsymbol{\alpha}}}{\Delta x}\left(\boldsymbol{F}_{j+1}^n - \boldsymbol{F}_j^n\right). \tag{22}$$

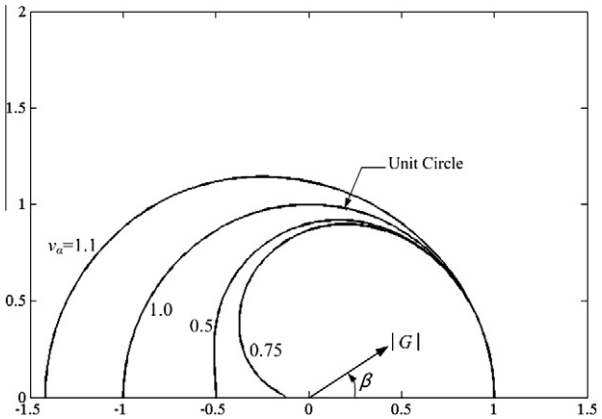

Fig. 2. Polar plot of G modulus.

Corrector:

$$\boldsymbol{E}_j^{n+1} = \frac{1}{2}\left[-\sum_{k=1}^{n+1}\omega_k^{\alpha}\boldsymbol{E}_j^{n+1-k} + \widetilde{\boldsymbol{E}}_j^{n+1} - \frac{\Delta t^{\alpha}}{\Delta x}\left(\widetilde{\boldsymbol{F}}_j^{n+1} - \widetilde{\boldsymbol{F}}_{j-1}^{n+1}\right)\right], \tag{23}$$

where the values with tilde ($\sim$) denote the predicted values computed from Eq. (22).

In order to perform the stability analysis for systems of equations and use the results of the stability analysis of scalar time-fractional conservation equation, we rewrite Eq. (21) as

$$\frac{\partial^{\alpha}\boldsymbol{E}}{\partial t^{\alpha}} + \left[\frac{\partial \boldsymbol{F}}{\partial \boldsymbol{E}}\right]\frac{\partial \boldsymbol{E}}{\partial x} = \boldsymbol{0} \tag{24}$$

or

$$\frac{\partial^{\alpha}\boldsymbol{E}}{\partial t^{\alpha}} + [A]\frac{\partial \boldsymbol{E}}{\partial x} = \boldsymbol{0}, \tag{25}$$

where $[\boldsymbol{A}]$ is called Jacobian matrix and is equal to $[\partial \boldsymbol{F}/\partial \boldsymbol{E}]$. Now, using a similar approach that we have employed for studying the stability of a linear scalar time-fractional equation and applying the GMcC scheme (22) and (23) on systems of Eq. (25), the following equation is obtained:

$$[\boldsymbol{G}] = \left|\frac{\boldsymbol{C}_{n+1}}{\boldsymbol{C}_0}\right| \leqslant \left|-[\boldsymbol{S}][\boldsymbol{A}]i\sin(\beta) + [\boldsymbol{I}] + ([\boldsymbol{S}][\boldsymbol{A}])^2(\cos(\beta) - [\boldsymbol{I}]) + \frac{1}{2}[\boldsymbol{S}][\boldsymbol{A}]\cos(\beta)\right|, \tag{26}$$

where $[\boldsymbol{G}]$ and $[\boldsymbol{I}]$ are amplification and identity matrix, respectively. The matrix $[\boldsymbol{S}]$ is the matrix of the ratio of time to space step sizes and is defined as

$$[\boldsymbol{S}] = \begin{bmatrix} \frac{\Delta t^{\alpha_1}}{\Delta x} & 0 & 0 \\ 0 & \ddots & 0 \\ 0 & 0 & \frac{\Delta t^{\alpha_m}}{\Delta x} \end{bmatrix}. \tag{27}$$

Comparing Eq. (26) with Eq. (20) we observe that Eq. (26) is the vectorial counterpart of Eq. (20) in which the constant c and $\Delta t^{\alpha}/\Delta x$ are replaced by $[\boldsymbol{A}]$ and $[\boldsymbol{S}]$, respectively. In other words, the CFL number $v_{\alpha} = c\Delta t^{\alpha}/\Delta x$ in the scalar time-fractional conservation equation is now replaced by *CFL matrix* $[\boldsymbol{v}_{\alpha}] = [\boldsymbol{S}][\boldsymbol{A}]$ in systems of time-fractional conservation equations.

By comparing Eq. (26) with Eq. (20) we find that stability is achieved when the largest eigenvalue of the CFL matrix $[\boldsymbol{v}_{\alpha}] = [\boldsymbol{S}][\boldsymbol{A}]$, λ_{max}, satisfies the following condition:

$$|\lambda_{\max}| \leqslant 1. \tag{28}$$

In this way, GMcC scheme is formulated for solving systems of time-fractional Eq. (21). Actually, the same approach of extending a numerical scheme from a single model equation to systems of equations which is very common in hyperbolic systems of equations has been now generalized for time-fractional equations. This offers us great opportunities for generalizing well-established approaches from classical conservation equations i.e. hyperbolic equations, to fractional conservation equations in future.

In the next section, we apply GMcC scheme (22) and (23) for solving the generalized Cattaneo equation which is a special case of systems of Eq. (21). The CFL number of Eq. (28) is also found for the generalized Cattaneo equation.

4. Numerical solution of generalized Cattaneo equation

In this section, we present the numerical solution of the generalized Cattaneo equation. In addition to GMcC scheme, we also use a totally implicit scheme in solving this equation.

4.1. Generalized MacCormack scheme

Having formulated the GMcC scheme for systems of time-fractional equations, in this section we formulate it for generalized Cattaneo equation. For this scheme, we use the idea of LOA for solving the generalized Cattaneo equation i.e. instead of eliminating flux term from the two Eqs. (2) and (9) and arriving at a single higher-order undecomposed governing Eq. (10), we solve a system of *two coupled* decomposed equations i.e. $m = 2$ in (21).

First, we rewrite system of governing Eqs. (9) and (2) in the following vector form:

$$\frac{\partial^{\beta}\boldsymbol{E}}{\partial t^{\beta}} + \frac{\partial \boldsymbol{F}}{\partial x} = \boldsymbol{H}, \tag{29}$$

where vectors $\boldsymbol{E}$, $\boldsymbol{F}$, $\boldsymbol{H}$ and $\boldsymbol{\beta}$ are the vector of conserved variable, flux, source term and order of differentiation, respectively, and for the system of Eqs. (9) and (2), they are defined as follows:

$$\boldsymbol{E} = \begin{bmatrix} f \\ u \end{bmatrix}, \quad \boldsymbol{F} = \begin{bmatrix} \frac{D}{\tau^{\alpha}} \cdot u \\ f \end{bmatrix}, \quad \boldsymbol{H} = \begin{bmatrix} \frac{-f}{\tau^{\alpha}} \\ 0 \end{bmatrix}, \quad \boldsymbol{\beta} = \begin{bmatrix} \alpha \\ 1 \end{bmatrix}. \tag{30}$$

Now, we formulate GMcC scheme for system of Eq. (29) in the following form:
Predictor:

$$\widetilde{\boldsymbol{E}}_j^{n+1} = -\sum_{k=1}^{n+1} \omega_k^{\alpha} \boldsymbol{E}_j^{n+1-k} - \frac{\Delta t^{\alpha}}{\Delta x}\left(\boldsymbol{F}_{j+1}^{n} - \boldsymbol{F}_j^{n}\right) + \Delta t^{\alpha} H_j^{n}. \tag{31}$$

Corrector:

$$\boldsymbol{E}_j^{n+1} = \frac{1}{2}\left[-\sum_{k=1}^{n+1} \omega_k^{\alpha} \boldsymbol{E}_j^{n+1-k} + \widetilde{\boldsymbol{E}}_j^{n+1} - \frac{\Delta t^{\alpha}}{\Delta x}\left(\widetilde{\boldsymbol{F}}_j^{n+1} - \widetilde{\boldsymbol{F}}_{j-1}^{n+1}\right) + \Delta t^{\alpha} \widetilde{\boldsymbol{H}}_j^{n+1}\right]. \tag{32}$$

In this way, knowing the values of $\boldsymbol{E}$, $\boldsymbol{F}$ and $\boldsymbol{H}$ at time step (n), the predicted values $(\tilde{})$ are calculated via Eq. (31) and the corrected values at time step $(n+1)$ consequently can be found via Eq. (32).

For the vectors defined in (30), the Jacobian matrix $[\boldsymbol{A}]$ and also the matrix $[\boldsymbol{S}]$ are found to be:

$$[\boldsymbol{A}] = \begin{bmatrix} 0 & \frac{D}{\tau^{\alpha}} \\ 1 & 0 \end{bmatrix}, \quad [\boldsymbol{S}] = \begin{bmatrix} \frac{\Delta t^{\alpha}}{\Delta x} & 0 \\ 0 & \frac{\Delta t}{\Delta x} \end{bmatrix}. \tag{33}$$

According to (33), the CFL matrix $[\boldsymbol{v}_{\alpha}] = [\boldsymbol{S}][\boldsymbol{A}]$ becomes:

$$[\boldsymbol{v}_{\alpha}] = \begin{bmatrix} 0 & \frac{D}{\tau^{\alpha}} \frac{\Delta t}{\Delta x} \\ \frac{\Delta t^{\alpha}}{\Delta x} & 0 \end{bmatrix}. \tag{34}$$

According to the discussion made in the previous section, GMcC scheme (31) and (32) for solving systems of Eq. (29) is stable when the largest eigenvalue of CFL matrix (34) is less than or equal 1. For the CFL matrix (34), the vector of eigenvalues is found to be:

$$[\boldsymbol{\lambda}] = \begin{bmatrix} \frac{\sqrt{\Delta t^{1+\alpha} \frac{D}{\tau^{\alpha}}}}{\Delta x} \\ -\frac{\sqrt{\Delta t^{1+\alpha} \frac{D}{\tau^{\alpha}}}}{\Delta x} \end{bmatrix}. \tag{35}$$

Therefore, GMcC scheme (31) and (32) for generalized Cattaneo Eq. (29) is stable when:

$$\lambda_{\max} = \frac{\sqrt{\Delta t^{1+\alpha} \frac{D}{\tau^{\alpha}}}}{\Delta x} \leqslant 1. \tag{36}$$

Two important results can be drawn from the obtained CFL number of (36). First, for the upper limiting case of α, i.e. $\alpha = 1$, the governing Eq. (29) reduce to classical Cattaneo equation and form two coupled hyperbolic equations. For this case, CFL number (36) reduces to $\lambda_{\max} = \Delta t\sqrt{D/\tau}/\Delta x \leqslant 1$ which is the CFL number for the classical MacCormack scheme used for solving systems of hyperbolic Eq. (29) with $\alpha = 1$. $\sqrt{D/\tau}$ is also the wave speed in classical Cattaneo equation. However, when α reduces from 1 and approaches to 0, the combined feature of the governing equations tends to pure diffusive nature. If we rewrite the CFL number in the following form, $\Delta t^{1+\alpha} \cdot D/\tau^{\alpha}/\Delta x^2 \leqslant 1$, we observe that for the limiting case of $\alpha = 0$, CFL number reduces to $D \cdot \Delta t/\Delta x^2 \leqslant 1$ which results in the conventional $O(\Delta x^2)$ time step for classical Fourier or Fick diffusion equations. Therefore, two limiting CFL numbers of hyperbolic and parabolic equations are correctly recovered from stability condition (36). In addition, GMcC scheme developed in this study can be used for solving any sets of coupled time-fractional equations that can be written in the vectorial form of (29). Also, the required CFL number can be easily found in the same way as is done in this section.

One of the great benefits of the idea of LOA is the simultaneous computation of the flux term (heat or mass flux) with the main variable with the same order of accuracy. This automatically eliminates the need of post-processing for computing the flux term. Another gain of this idea is the possibility of using higher-order *explicit* schemes for solving anomalous diffusion equations.

It should be mentioned that single predictor Eq. (31) can be viewed as fractional upwind scheme and can be used for solving Eq. (29). Since this fractional upwind scheme by itself does not introduce any important feature, it is not considered as a separate scheme in the present study. However, a reasonable combination of this first-order fractional upwind scheme with a higher-order scheme may result in developing more efficient schemes. This feature is well established in solving well-known hyperbolic equations such as Euler, shallow water and thermal wave equations. In fact, the idea of writing the governing equations as a system of time-fractional conservation equations offers us great opportunities for generalizing higher-order efficient numerical schemes which are used for system of hyperbolic equations. This has been successfully done for the case of MacCormack scheme in the present study.

For treating the boundary conditions for solving Eqs. (31) and (32), zeroth order extrapolation technique using conserved variables [24] has been employed.

4.2. Totally implicit scheme

For the numerical formulation of totally implicit scheme HOA is used, i.e. solving Eq. (10) instead of a system of two coupled equations. Since, the Caputo definition has been used in Eq. (10) we first need to discretize the time fractional derivative and then proceed with the totally implicit formulation of Eq. (10). In [14,20], the authors derived a discretization form of Caputo-based fractional derivative for the case of $0 < \alpha < 1$. However, since the order of time fractional derivative in Eq. (10) is greater than 1, the discretization formulas presented in Refs. [14,20] cannot be employed in the present study. Therefore, we first find an approximation for the Caputo-based time fractional derivative with the fractional order $1 < \beta \leqslant 2$.

4.2.1. Numerical approximation of Caputo-based fractional derivative

Here, we first begin with the definition of fractional derivative based on Caputo definition. For $1.0 < \beta \leqslant 2.0$, Caputo definition of time fractional derivative gives:

$$\frac{\partial^\beta u}{\partial t^\beta} = \frac{1}{\Gamma(2-\beta)} \int_0^{t_n} \frac{\partial^2 u}{\partial t^2} (t_n - s)^{1-\beta} ds. \tag{37}$$

To obtain the fractional time derivative discretization, we first replace the integral term in Eq. (37) with a summation, then the second-order time derivative in Eq. (37) is approximated by second-order backward difference to find the final discretization formulation in the time in the following form:

$$\begin{aligned}
\frac{\partial^\beta u}{\partial t^\beta} &= \frac{1}{\Gamma(2-\beta)} \sum_{k=1}^{n} \int_{t_{k-1}}^{t_k} \frac{\partial^2 u}{\partial t^2} (t_n - s)^{1-\beta} ds = \frac{1}{\Gamma(2-\beta)} \sum_{k=1}^{n} \int_{t_{k-1}}^{t_k} \left(\frac{u(x,t_k) - 2u(x,t_{k-1}) + u(x,t_{k-2})}{\Delta t^2} \right) (t_n - s)^{1-\beta} ds \\
&= \frac{1}{\Gamma(2-\beta)} \sum_{k=1}^{n} \left(\frac{u(x,t_k) - 2u(x,t_{k-1}) + u(x,t_{k-2})}{\Delta t^2} \right) \times \int_{t_{k-1}}^{t_k} (t_n - s)^{1-\beta} ds \\
&= \frac{1}{\Gamma(2-\beta)} \sum_{k=1}^{n} \left(\frac{u(x,t_k) - 2u(x,t_{k-1}) + u(x,t_{k-2})}{\Delta t^2} \right) \times \left[-(t_n - t_k)^{2-\beta} + (t_n - t_{k-1})^{2-\beta} \right] \times \frac{1}{2-\beta} \\
&= \frac{1}{\Gamma(2-\beta)} \frac{1}{2-\beta} \sum_{k=1}^{n} \left(\frac{u(x,t_k) - 2u(x,t_{k-1}) + u(x,t_{k-2})}{\Delta t^2} \right) \times \left[(n-k+1)^{2-\beta} - (n-k)^{2-\beta} \right] \times \Delta t^{2-\beta} \\
&= \frac{1}{\Gamma(2-\beta)} \frac{1}{2-\beta} \frac{1}{\Delta t^\beta} \sum_{k=1}^{n} (u(x,t_k) - 2u(x,t_{k-1}) + u(x,t_{k-2})) \times \left[(n-k+1)^{2-\beta} - (n-k)^{2-\beta} \right]
\end{aligned} \tag{38}$$

Setting:

$$\sigma_\beta = \frac{1}{\Gamma(2-\beta)} \frac{1}{2-\beta} \frac{1}{\Delta t^\beta},$$

and shifting the indices in the summation and setting again:

$$\omega_k^\beta = k^{2-\beta} - (k-1)^{2-\beta}$$

leads to:

$$\frac{\partial^\beta u(x,t_n)}{\partial t^\beta} = \sigma_\beta \cdot \sum_{k=1}^{n} \omega_k^\beta \cdot \left(u_j^{n-k+1} - 2u_j^{n-k} + u_j^{n-k-1} \right). \tag{39}$$

Eq. (39) is the discretization form of Caputo-based time fractional derivative in the case of $1.0 < \beta \leqslant 2.0$.

4.2.2. Implicit finite difference scheme

We discretize the three terms of Eq. (10) in the following totally implicit form:

$$\left. \frac{\partial u}{\partial t} \right|_j^n = \frac{3u_j^n - 4u_j^{n-1} + u_j^{n-2}}{2\Delta t},$$

$$\left. \frac{\partial^{1+\alpha} u}{\partial t^{1+\alpha}} \right|_j^n = \left. \frac{\partial^\beta u}{\partial t^\beta} \right|_j^n = \sigma_\beta \cdot \sum_{k=1}^{n} \omega_k^\beta \cdot \left(u_j^{n-k+1} - 2u_j^{n-k} + u_j^{n-k-1} \right),$$

$$\left. \frac{\partial^2 u}{\partial x^2} \right|_j^n = \frac{u_{j+1}^n - 2u_j^n + u_{j-1}^n}{\Delta x^2}.$$

We now arrange the discretization equation in the following form remembering that $\omega_1^{1+\alpha} = 1$:

$$\left(-\frac{1}{\Delta x^2}\right)u_{j+1}^n + \left(\frac{3}{2\Delta t} + \sigma_\beta + \frac{2}{\Delta x^2}\right)u_j^n + \left(-\frac{1}{\Delta x^2}\right)u_{j-1}^n = 2\sigma_\beta \cdot u_j^{n-1} - \sigma_\beta \cdot u_j^{n-2} - \sigma_\beta \cdot \sum_{k=2}^{n} \omega_k^\beta \cdot \left(u_j^{n-k+1} - 2u_j^{n-k} + u_j^{n-k-1}\right) + \frac{2}{\Delta t}u_j^{n-1} - \frac{1}{2\Delta t}u_j^{n-2}. \tag{40}$$

For solving Eq. (40), we need to solve a tridiagonal system of linear equations in each time step which can be easily done via a TDMA solver [24]. In the next section, numerical tests demonstrate the convergence rate of $O(\Delta t, \Delta x^2)$ for fully implicit scheme.

From the stability point of view, the authors were not able to prove the stability of Eq. (40) by using Von Neumann stability criterion employed in the previous section for the generalized MacCormack scheme but numerous numerical tests for wide range of existing parameters i.e. time-step size, grid size and α, have been performed and no symptoms of numerical instability have been observed. Thus, unconditional stability of fully implicit formulation (40) is likely but is not proven.

5. Numerical test

Consider the generalized Cattaneo equation with the following boundary and initial conditions:

$$\begin{aligned} &u(0,t) = 1.0, \quad t > 0, \\ &u(1,t) = 0, \quad t > 0, \\ &u(x,0) = 0, \end{aligned} \tag{41}$$

$$\left.\frac{\partial u}{\partial t}\right|_{t=0} = 0. \tag{42}$$

Boundary conditions (41) impose a unit step change in the temperature of a medium from its initial conditions. For simplicity, all parameters in generalized Cattaneo equation are set to unity. It should be reminded that by generalized Cattaneo equation we mean either two coupled Eqs. (2)–(9) in decomposed form used in GMcC scheme or one single Eq. (10) used in FI scheme.

The exact solution of the problem is found through Laplace transform and Riemann sum approximation for Laplace inversion. The main advantage of this technique is the existence of only a single summation compared with most of the analytical solutions of fractional partial differential equations which contain multiple summation terms that make numerical processing more difficult than that used in this technique.

Taking the Laplace transform of Eqs. (10) and (41) and taking into account the initial conditions (42) gives:

$$s \cdot \bar{u}(x,s) + s^{1+\alpha} \cdot \bar{u}(x,s) = \frac{d^2\bar{u}(x,s)}{dx^2} \tag{43}$$

$$\begin{aligned} &\bar{u}(0,s) = \frac{1.0}{s}, \\ &\bar{u}(1,s) = 0. \end{aligned} \tag{44}$$

Now solving Eqs. (43) and (44) results in

$$\bar{u}(x,s) = -\frac{e^{(-1+x)\sqrt{s(1+s^\alpha)}} - e^{-(-1+x)\sqrt{s(1+s^\alpha)}}}{s\left(e^{\sqrt{s(1+s^\alpha)}} - e^{-\sqrt{s(1+s^\alpha)}}\right)}. \tag{45}$$

For the purpose of Laplace inversion and finding $u(x,t)$, we have employed Riemann sum approximation technique. To do this, we insert Eq. (45) into:

$$u(x,t) = \frac{e^{\gamma t}}{t}\left[\frac{1}{2}\bar{u}(x, s=\gamma) + Re\sum_{n=1}^{N}\bar{u}\left(x, s = \gamma + \frac{in\pi}{t}\right)(-1)^n\right], \tag{46}$$

where the value of γ is equal to $(2 + e)/t$ and Re is the real part of the summation. In Fig. 3, exact solution has been plotted for some typical values of α at time $t = 0.4$.

As can be seen from Fig. 3, as the order of differentiation α approaches 1, hyperbolicity dominates diffusivity which allows the propagation of step perturbation of the left boundary in the medium. For the limiting case of $\alpha = 1$, the governing equation becomes damped wave equation for which the step perturbation propagates as a sharp discontinuity in the medium.

In order to compare the two numerical schemes more qualitatively, we calculate the error norms of both generalized MacCormack and fully implicit schemes relative to the exact solution. Two error norms have been used in this study: E_{L1} norm and $E_{L\infty}$ norm which are defined respectively as

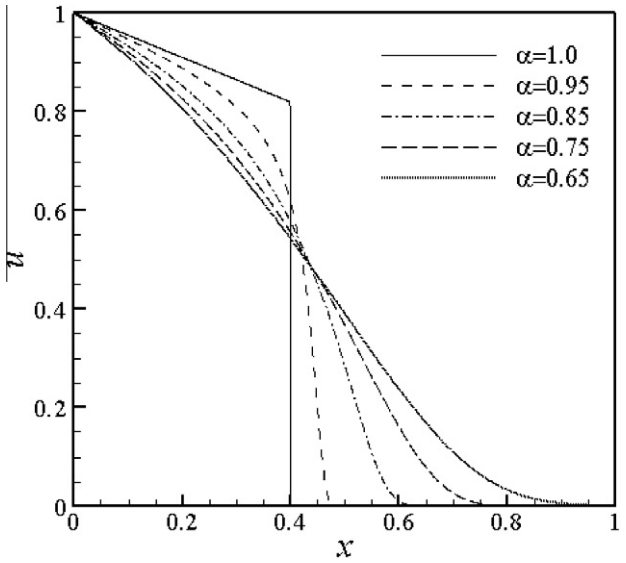

Fig. 3. Exact solution of step perturbation problem at $t = 0.4$.

$$E_{L_1} = \frac{1}{N}\sum_{i=1}^{N} E(i), \tag{47}$$

$$E_{\infty} = \max\left(E(i)\right)|_{i=1\ldots N}, \tag{48}$$

where

$$E(i) = |u(i) - U(i)|,$$

in which $u(i)$ is the numerical approximation, whereas $U(i)$ is the exact solution at each grid point.

Tables 1 and 2 show the global error and spatial EOC for FI scheme for both norms. From Tables 1 and 2 we observe that spatial EOC for fully implicit scheme is 2. Tables 3 and 4 show the global EOC for GMcC scheme in the case of L_1-norm and L_∞-norm, respectively. Like the fully implicit case, second-order global rate of convergency is achieved. We can observe that for a specified α, calculated EOC based on L_1-norm is slightly higher than that based on L_∞-norm specially near $\alpha = 1.0$. The reason returns to the very definition of these two norms. L_∞-norm considers the maximum error whereas L_1-norm is an average of all errors in the domain. Thus, in L_1-norm the negative effect of high errors near the possible discontinuities of the solution is smoothed by the small errors in other parts of the solution domain. For α smaller than 0.6, since the solution becomes completely smooth, EOC remains constant and 2.

To find the temporal EOC, space step Δx should be chosen sufficiently small in order to prevent entering the effect of spatial discretization error in the calculation. Since fully implicit scheme is unconditionally stable, in choosing triple time step sizes and also sufficiently small Δx, we do not face any problem. However, this is not the case for GMcC scheme for which we are also restricted to satisfying the stability condition. Therefore, for each α in GMcC scheme, Δx has been chosen sufficiently small for avoiding both spatial discretization error and also contamination of round off error.

From Tables 5 and 6, we can conclude that fully implicit scheme is globally first order convergent in time. However, from Tables 7–9, we observe that temporal rate of convergency for GMcC scheme is around $(1 + \alpha)$ for three different values of α

Table 1
Spatial global L_1 error and EOC for fully implicit scheme at $t = 0.4$ for $\Delta t = 0.00002$.

α	E_{L1}			L_1 rate
0.9	$N_x = 40$ 4.67E−03	$N_x = 80$ 1.25E−03	$N_x = 160$ 3.62E−04	1.85
0.8	$N_x = 10$ 1.24E−02	$N_x = 20$ 3.44E−03	$N_x = 40$ 9.07E−04	1.89
0.7	$N_x = 10$ 5.12E−03	$N_x = 20$ 1.29E−03	$N_x = 40$ 3.18E−04	2.00
0.6	$N_x = 10$ 1.90E−03	$N_x = 20$ 4.66E−04	$N_x = 40$ 1.11E−04	2.05

Table 2
Spatial global L_∞ error and EOC for fully implicit scheme at $t = 0.4$ for $\Delta t = 0.00002$.

α	E_{L1}			L_∞ rate
0.9	$N_x = 40$ 4.03E−02	$N_x = 80$ 1.34E−02	$N_x = 160$ 4.85E−03	1.53
0.8	$N_x = 10$ 4.85E−02	$N_x = 20$ 1.75E−02	$N_x = 40$ 5.39E−03	1.58
0.7	$N_x = 10$ 1.40E−02	$N_x = 20$ 4.79E−03	$N_x = 40$ 1.43E−03	1.65
0.6	$N_x = 10$ 5.42E−03	$N_x = 20$ 1.28E−03	$N_x = 40$ 3.61E−04	1.95

Table 3
Spatial global L_1 error and EOC for GMcC scheme at $t = 0.4$ for $\Delta t = 0.0001$.

α	E_{L1}			L_1 rate
0.9	$N_x = 80$ 5.18E−03	$N_x = 160$ 1.22E−03	$N_x = 320$ 2.98E−04	2.06
0.8	$N_x = 40$ 3.99E−03	$N_x = 80$ 9.40E−04	$N_x = 160$ 2.20E−04	2.09
0.7	$N_x = 20$ 5.93E−03	$N_x = 40$ 1.41E−03	$N_x = 80$ 3.03E−04	2.14
0.6	$N_x = 20$ 2.46E−03	$N_x = 40$ 4.64E−04	$N_x = 80$ 1.21E−04	2.17

Table 4
Spatial global L_∞ error and EOC for GMcC scheme at $t = 0.4$ for $\Delta t = 0.0001$.

α	E_{L1}			L_∞ rate
0.9	$N_x = 80$ 4.39E−02	$N_x = 160$ 1.66E−02	$N_x = 320$ 3.88E−03	1.75
0.8	$N_x = 40$ 2.24E−02	$N_x = 80$ 5.75E−03	$N_x = 160$ 1.29E−03	2.06
0.7	$N_x = 20$ 2.16E−02	$N_x = 40$ 4.84E−03	$N_x = 80$ 1.08E−03	2.16
0.6	$N_x = 20$ 7.24E−03	$N_x = 40$ 1.26E−03	$N_x = 80$ 3.40E−04	2.21

Table 5
Temporal Global L_1 error and L_1 convergence rate for fully implicit scheme at $t = 0.4$ for $\Delta x = 0.01$.

α	E_{L1}			L_1 rate
	$N_t = 40$	$N_t = 80$	$N_t = 160$	
0.9	2.15E−02	1.22E−02	6.72E−03	0.84
0.8	1.56E−02	8.11E−03	4.10E−03	0.96
0.7	1.28E−02	6.47E−03	3.21E−03	1.00
0.6	1.10E−02	5.48E−03	2.71E−03	1.01

Table 6
Temporal Global L_∞ error and L_∞ convergence rate for fully implicit scheme at $t = 0.4$ for $\Delta x = 0.01$.

α	$E_{L\infty}$			L_∞ rate
	$N_t = 40$	$N_t = 80$	$N_t = 160$	
0.9	1.19E−01	7.48E−02	4.42E−02	0.71
0.8	6.03E−02	3.20E−02	1.60E−02	0.96
0.7	3.67E−02	1.83E−02	8.96E−03	1.02
0.6	2.54E−02	1.25E−02	6.14E−03	1.02

Table 7
Temporal Global Error and EOC for $\alpha = 0.8$ and $N_x = 250$ for GMcC scheme at $t = 0.4$.

N_t	E_{L1}	L_1 rate	$E_{L\infty}$	L_∞ rate
400	9.67E−04	–	4.16E−03	–
800	3.28E−04	1.56	1.66E−03	1.33
1600	8.48E−05	1.95	4.72E−04	1.81

Table 8
Temporal Global Error and EOC for $\alpha = 0.7$ and $N_x = 200$ for GMcC scheme at $t = 0.4$.

N_t	E_{L1}	L_1 rate	$E_{L\infty}$	L_∞ rate
800	4.57E−04	–	1.24E−03	–
1600	1.58E−04	1.53	4.90E−04	1.34
3200	4.32E−05	1.87	1.53E−04	1.68

Table 9
Temporal Global Error and EOC for $\alpha = 0.6$ and $N_x = 125$ for GMcC scheme at $t = 0.4$.

N_t	E_{L1}	L_1 rate	$E_{L\infty}$	L_∞ rate
1333	3.62E−04	–	7.46E−04	–
2666	1.93E−04	0.91	4.34E−04	0.78
5332	6.62E−05	1.55	1.76E−04	1.30

Table 10
Performance results for GMcC scheme for pulse perturbation, $N = 201$.

α	Δt	E_{L1}	$E_{L\infty}$	CPU time (s)
0.95	3.39E−03	5.80E−03	1.18E−01	0.11
0.9	2.47E−03	2.95E−03	3.72E−02	0.17
0.85	1.73E−03	1.95E−03	1.58E−02	0.36
0.8	1.17E−03	6.09E−04	4.79E−03	0.73
0.75	7.43E−04	4.80E−04	2.54E−03	1.80
0.7	4.44E−04	2.50E−04	2.54E−03	5.19
0.6	1.23E−04	5.60E−05	2.54E−03	76.19

Table 11
Performance results for fully implicit scheme for pulse perturbation, $N = 201$.

α	Δt	E_{L1}	$E_{L\infty}$	CPU time (s)
0.95	2.00E−03	1.15E−02	1.89E−01	16.44
0.9	2.00E−03	5.71E−03	7.25E−02	16.41
0.85	2.00E−03	3.28E−03	3.25E−02	16.50
0.8	2.00E−03	2.34E−03	1.69E−02	16.50
0.75	2.00E−03	1.98E−03	9.92E−03	16.48
0.7	2.00E−03	1.78E−03	6.47E−03	16.48
0.6	2.00E−03	1.57E−03	3.52E−03	16.56

namely 0.8, 0.7 and 0.6. Compared with previously introduced schemes, GMcC scheme has a very good temporal order of convergency which is due to its predictor–corrector formulation.

In order to quantify some features of computational efficiencies of GMcC and FI schemes more precisely, the solution of generalized Cattaneo equation under the following pulse condition at $x = 0$ has been sought:

$$\begin{cases} u(x=0) = 1.0, & 0 < t \leqslant 0.04, \\ u(x=0) = 0.0, & 0.04 < t, \\ u(1,t) = 0, & 0 < t. \end{cases} \tag{49}$$

For both schemes, the same number of grid points viz. $N = 201$, has been used and the results are calculated to a fixed final time of $t = 0.4$ s. The results of Tables 10 and 11 show that GMcC scheme outperforms FI scheme with regard to the consumption of CPU time for a complete simulation to $t = 0.4$ s, specially for α near 1, in addition to smaller norm errors. This great

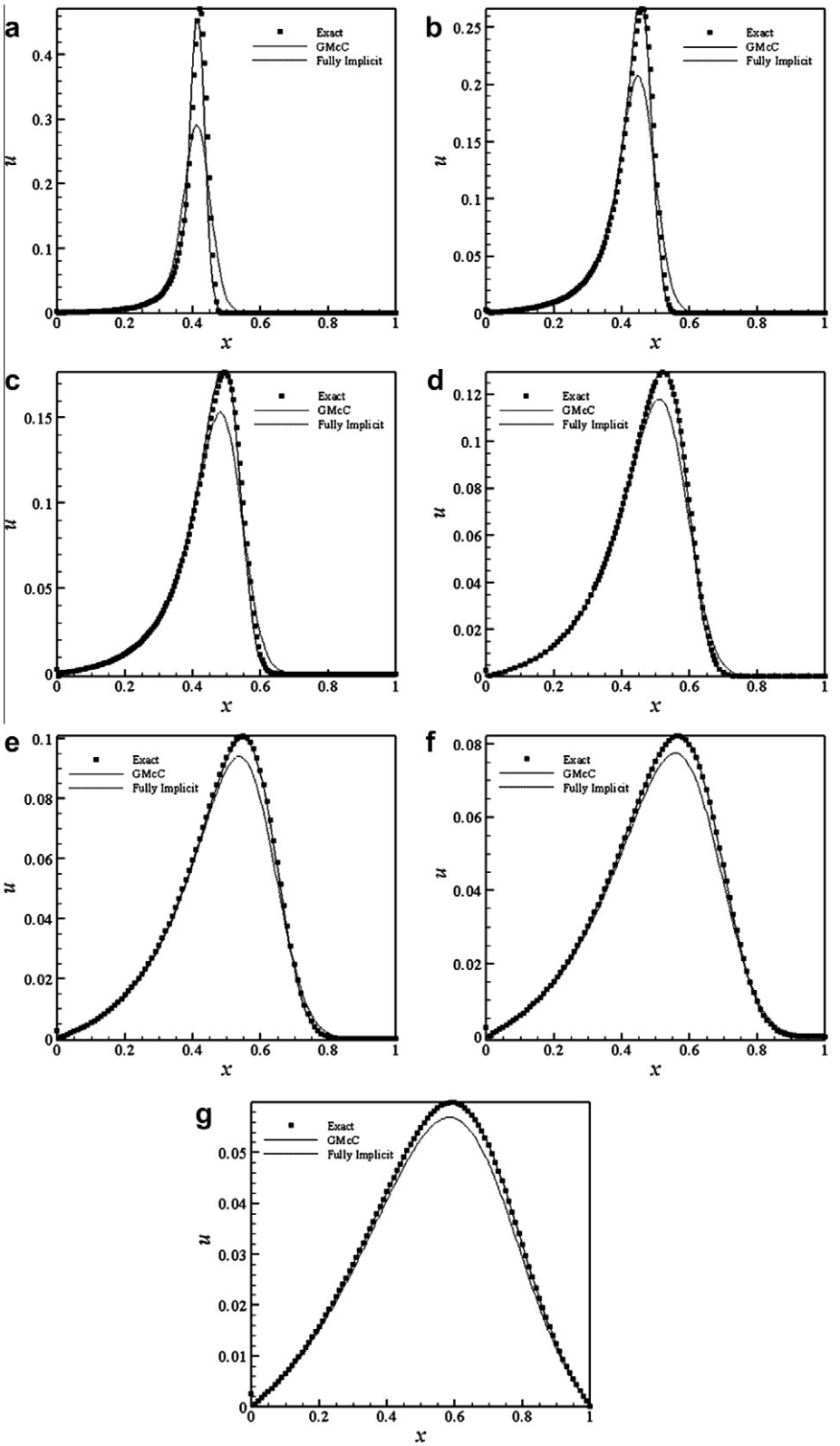

Fig. 4. Temperature distribution for pulse perturbation problem: (a) $\alpha = 0.95$, (b) $\alpha = 0.9$, (c) $\alpha = 0.85$, (d) $\alpha = 0.8$, (e) $\alpha = 0.75$, (f) $\alpha = 0.7$, and (g) $\alpha = 0.6$.

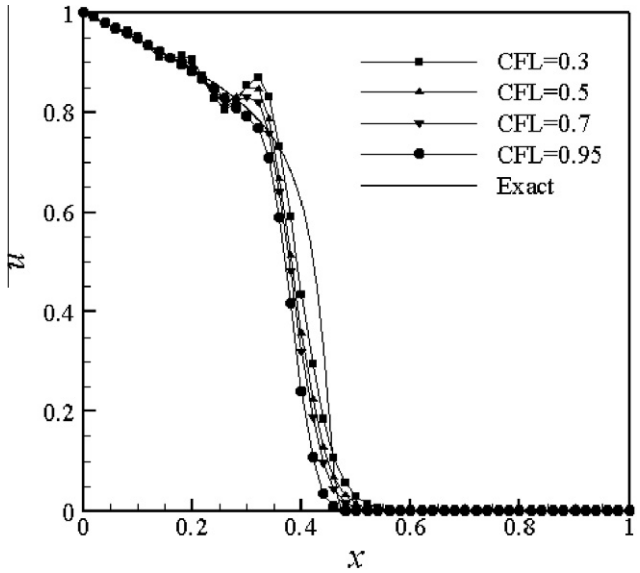

Fig. 5. Effect of CFL number on spurious oscillations in GMcC scheme.

speed-up in the CPU time is because of the explicit nature of GMcC scheme and also LOA that has been used in its formulation. It should be remembered that this high speed-up in CPU time has been achieved despite the computation of an extra term (flux term) in each time step. However, for $\alpha = 0.6$ we observe that CPU time of GMcC scheme dramatically increases which is due to its stability condition. On the other hand, since Δx and Δt are fixed irrespective to α, CPU time of FI scheme is fixed. Also, the graphical results in Fig. 4 show that GMcC scheme is an efficient scheme in capturing the discontinuities from both sides of pulse perturbation problem of Eq. (49).

One interesting property of GMcC scheme is that, like integer-order MacCormack scheme, it works well with higher values of CFL number. In integer-order MacCormack scheme, as we get far from CFL = 1.0, the number and the amplitude of the spurious oscillations near a discontinuity increase. In order to show that this property is also valid for GMcC scheme, we repeat the numerical test of step perturbation problem for $\alpha = 0.95$ with large mesh sizes. In Fig. 5, we can see that as CFL number decreases, the frequency and amplitude of spurious oscillations in the numerical solution of GMcC scheme increase. It is also observable from Fig. 4 that FI scheme is of diffusive nature in contrast to dispersive behavior of GMcC scheme near the discontinuities. Both of these features vanish as the order of differentiability α, i.e. hyperbolicity, decreases from 1.

From the obtained results, we can draw the following conclusions: first, when α is near 1 and the governing equation allows the propagation of discontinuity in the medium, GMcC scheme is completely preferred to fully implicit scheme. The reason returns to higher rate of convergency for GMcC scheme in comparison to fully implicit scheme. In other words, in using fully implicit scheme for α near 1, as Fig. 4 shows, we need to use finer mesh in order to capture the discontinuity. Subsequently, because of the implicit nature of the scheme, computational costs greatly increase. This feature is observable from the results of Table 11. Second, for α sufficiently far from 1 and in the absence of non-smooth solution, fully implicit scheme can be preferred to GMcC scheme because of the stability limitation of GMcC scheme. As α becomes smaller, stability region of GMcC scheme shrinks and for a fixed Δx, Δt becomes very small which in turn increases the computational time. This feature is also evident from Table 10. Therefore, for lower values of α, resorting to fully implicit scheme seems to be necessary.

6. Concluding remarks

In the present study, the generalized Cattaneo equation based on Caputo definition has been first recovered by applying generalized Taylor formula on single delay equation. Then, based on two different formulating ideas namely lower-order and higher-order approaches, two finite difference schemes namely an explicit predictor–corrector and a one-step totally implicit scheme have been developed. LOA enables us to compute the flux term simultaneously with the main variable. For the latter which has been called generalized MacCormack scheme, stability has been investigated through Fourier method and the corresponding CFL number has been derived. For fully implicit scheme, numerical tests suggest unconditional stability but it has not been proven. The spatial and temporal experimental orders of convergencies of both schemes have been obtained through a numerical test. It was found that both schemes are second-order accurate in space. For temporal rate of convergency, fully implicit scheme is first order accurate while the rate of convergency for generalized MacCormack scheme is $(1 + \alpha)$. Then, the domain of applicability of both schemes has been discussed and it was proposed that for α near 1, GMcC

scheme be used because of its explicit formulation, higher rate of convergency and discontinuity capturing capabilities. While for lower values of α, because of the diffusion dominant nature of the governing equations, we resort to fully implicit scheme.

Treating the generalized Cattaneo model through fractional Taylor series expansion and formulating it based on LOA can have applicability in other fractional diffusion equations. In the same way as for a set of pure hyperbolic equations, solving a set of low-order fractional equations may have tremendous benefits compared to solving a higher-order fractional diffusion equation.

The way of treating governing equations as a system of time-fractional conservation equations offers us great advantage of generalizing efficient and high-order numerical schemes of classical conservation equations to fractional ones. The generalization of classical MacCormack scheme in the present study paves the way for developing new and higher-order numerical methods for anomalous diffusion equations in future.

References

[1] W. Kaminski, Hyperbolic heat conduction equation for materials with a nonhomogeneous inner structure, ASME J. Heat Transfer 112 (1990) 555–560.
[2] K. Mitra, A. Kumar, A. Vedavarz, M.K. Moallemi, Experimental evidence of hyperbolic heat conduction in processed meat, ASME J. Heat Transfer 117 (1995) 568–573.
[3] P.J. Antaki, Importance of nonFourier heat conduction in solid-phase reactions, Combust. Flame 112 (1998) 329–341.
[4] H. Gomez, I. Colominas, F. Navarrina, M. Casteleiro, A mathematical model and a numerical model for hyperbolic mass transport in compressible flows, Heat Mass Transfer 45 (2008) 219–226.
[5] A. Compte, R. Metzler, The generalized Cattaneo equation for the description of anomalous transport processes, J. Phys. A: Math. Gen. 30 (1997) 7277–7289.
[6] F.J. Valdes-Parada, J.A. Ochoa-Tapia, J.A. Ochoa-Tapia, Effective medium equation for fractional Cattaneo's diffusion and heterogeneous reaction in disordered porous media, Physica A 369 (2006) 318–328.
[7] I. Podlubny, Fractional Differential Equations, Academic Press, New York, 1999.
[8] R.L. Magin, Fractional Calculus in Bioengineering, Begell House, Inc., 2006.
[9] E. Di Giuseppe, M. Moroni, M. Caputo, Flux in porous media with memory: models and experiments, Transport Porous Med. (2009), doi:10.1007/s11242-11,009-19456-11244.
[10] T.A.M. Langlands, B.I. Henry, The accuracy and stability of an implicit solution method for the fractional diffusion equation, J. Comput. Phys. 205 (2005) 719–736.
[11] K. Oldham, J. Spanier, The Fractional Calculus: Theory and Applications of Differentiation and Integration to Arbitrary Order, Academic Press, New York, London, 1974.
[12] S.B. Yuste, L. Acedo, An explicit finite difference method and a new Von Neumann-type stability analysis for fractional diffusion equations, SIAM J. Numer. Anal. 42 (2005) 1862–1874.
[13] S.B. Yuste, Weighted average finite difference methods for fractional diffusion equations, J. Comput. Phys. 216 (2006) 264–274.
[14] Y. Lin, C. Xu, Finite difference/spectral approximations for the time–fractional diffusion equation, J. Comput. Phys. 225 (2007) 1533–1552.
[15] W. Deng, Numerical algorithm for the time fractional Fokker–Planck equation, J. Comput. Phys. 227 (2007) 1510–1522.
[16] K. Diethelm, N.J. Ford, A.D. Freed, Detailed error analysis for a fractional Adams method, Numer. Algorithms 36 (2004) 31–52.
[17] K. Diethelm, N.J. Ford, A.D. Freed, A predictor–corrector approach for the numerical solution of fractional differential equations, Nonlinear Dynam. 29 (2002) 3–22.
[18] C.M. Chen, F. Liu, I. Turner, V. Anh, A Fourier method for the fractional diffusion equation describing sub-diffusion, J. Comput. Phys. 227 (2007) 886–897.
[19] R. Scherer, S.L. Kalla, L. Boyadjiev, B. Al-Saqabi, Numerical treatment of fractional heat equations, Appl. Numer. Math. 58 (2008) 1212–1223.
[20] D.A. Murio, Implicit finite difference approximation for time fractional diffusion equations, Comput. Math. Appl. 56 (2008) 1138–1145.
[21] M. Cui, Compact finite difference method for the fractional diffusion equation, J. Comput. Phys. 228 (2009) 7792–7804.
[22] D.Y. Tzou, A unified field approach for heat conduction from macro- to micro-scales, ASME J. Heat Transfer 117 (1995) 8–16.
[23] Z.M. Odibat, N.T. Shawagfeh, Generalized Taylor's formula, Appl. Math. Comput. 186 (2007) 286–293.
[24] J.C. Tannehill, D.A. Anderson, R.H. Pletcher, Computational Fluid Mechanics and Heat Transfer, second ed., Taylor and Francis, Washington, DC, 1997.